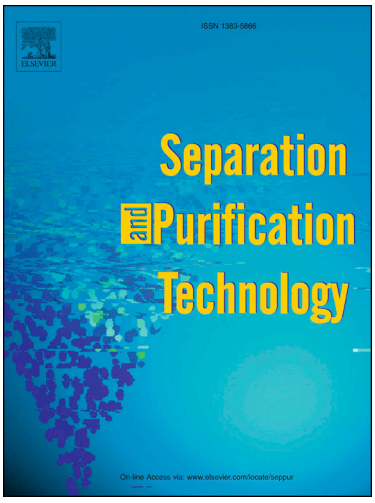

Permeability dependencies on the carrier concentration and membrane viscosity for Y(III) and Eu(III) transport by using liquid membranes

S. Pavón, A. Fortuny, M.T. Coll, M. Bertau, A.M. Sastre

PII: S1383-5866(19)33964-4
DOI: https://doi.org/10.1016/j.seppur.2020.116573
Reference: SEPPUR 116573

To appear in: *Separation and Purification Technology*

Received Date: 6 September 2019
Revised Date: 9 January 2020
Accepted Date: 14 January 2020

Please cite this article as: S. Pavón, A. Fortuny, M.T. Coll, M. Bertau, A.M. Sastre, Permeability dependencies on the carrier concentration and membrane viscosity for Y(III) and Eu(III) transport by using liquid membranes, *Separation and Purification Technology* (2020), doi: https://doi.org/10.1016/j.seppur.2020.116573

Permeability dependencies on the carrier concentration and membrane viscosity for Y(III) and Eu(III) transport by using liquid membranes

S. Pavón[a,b], A. Fortuny[a], M.T. Coll[c], M. Bertau[b], A.M. Sastre[d].

[a]*Chemical Engineering Department, EPSEVG, Universitat Politècnica de Catalunya, Víctor Balaguer 1, 08800 Vilanova i la Geltrú, Spain.*

[b]*Institute of Chemical Technology, TU Bergakademie Freiberg, Leipziger Straße 29, 09599 Freiberg, Germany.*

[c]*Agri-Food Engineering and Biotechnology Department, ESAB, Universitat Politècnica de Catalunya, Esteve Terrades 8, 08860 Castelldefels, Spain.*

[d]*Chemical Engineering Department, ETSEIB, Universitat Politècnica de Catalunya, Diagonal 647, 08028 Barcelona, Spain.*

ABSTRACT

The recovery of Y(III) and Eu(III) from fluorescent lamp leachates via supported liquid membranes using Cyanex 923 as a carrier has been studied. The results reveal that the transport process is mainly controlled by the diffusion or the viscosity of the organic phase depending on the carrier concentrations. Furthermore, this paper compares the transport model for flat sheet supported liquid membranes and hollow fibre renewal liquid membranes regarding both REEs in nitrate media. The model allows foreseeing the permeability coefficients for these REEs as a function of the organic phase variables. This study reveals furthermore, that the difference on the permeability coefficients between both membranes correlates to their structural characteristics, e.g. tortuosity, thickness and porosity.

Keywords

REE permeability coefficient; Supported liquid membrane; Hollow fibre renewal liquid membrane; REE recovery; Cyanex 923;

1. Introduction

Rare earths elements (REEs) have been widely used in advanced technologies due to their physical and chemical characteristics. The growing consumption of these metals will not change in the near future, because of their indispensable role in the products of electronic devices, electric and hybrid-electric vehicles and permanent magnets for wind turbines [1]. Since the content of REEs in phosphors of lamps can reach 27.9% [2], the processing of their waste streams and therefore, the use of this end-of-life products as feasible metal raw materials provides a promising alternative to recover and recycle REEs.

Red phosphors Y_2O_3:Eu^{3+} (YOX), blue phosphors $BaMgAl_{10}O_{17}$:Eu^{2+} (BAM) and green phosphors $LaPO_4$:Ce^{3+},Tb^{3+} (LAP), (Gd,Mg)B_5O_{12}:Ce^{3+},Tb^{3+} (CBT), (Ce,Tb)$MgAl_{11}O_{19}$ (CAT) are the three main different phosphors in fluorescent lamps, where the former contains the highest amount of REEs (55%) [3]. Moreover, since yttrium and europium are also the REEs with the highest content in this halophosphate phosphors (rich in YOX), these metals have been targeted in this investigation.

Despite the fact that many researches focus on the REEs recovery from the end-of-life products, industrial-scale applications are not wide spread. Solvent extraction is the most common technique to recover and

separate REEs although the consumption of organic solvents in large amounts as diluents is problematic [4]. Moreover, solvent extraction technique is less efficient for the separation of metal ions and pre-concentration compared to membrane separation processes, as membranes have the benefit of fast and selective ion transport due their large mass transfer interfacial areas [5].

There are a lot of liquid membrane types, which have high selectivity consisting of a supported or unsupported liquid phase serving as a membrane barrier between two phases of aqueous solutions. Emulsion liquid membrane (ELM) and immobilized liquid membrane, also known as supported liquid membrane (SLM), are the two main types of liquid membranes. ELMs are produced by forming a stable emulsion between two immiscible phases, followed by dispersion of this emulsion into a third. One disadvantage of this liquid membrane is the fragile membrane, which can break resulting in a leakage of aqueous droplets into the feed stream reducing the separation efficiency [6]. To avoid this problem, SLMs are used since the liquid membrane phase is an organic liquid imbedded in pores of a microporous support. Although there is a great number of SLMs, such as flat sheet supported liquid membranes (FSSLM), hollow fibre supported liquid membranes (HFSLM), hollow fibre renewal liquid membranes (HFRLM), etc. only some of them are suitable to be scaled-up because of their membrane stability problems [7]. SLMs without renewal configuration suffer a gradual loss of the organic membrane phase to the aqueous feed and stripping solutions. Emulsification at the membrane aqueous interfaces and the differences of the osmotic pressure across the membrane favour the organic phase losses [8]. Thus, the renewal configuration offers several potential advantages; high mass transfer rate, long-time stability of the liquid membrane, no leakage between the phases, low extractant consumption, wide range of operating parameters and easy scale-up [9–12].

Wannachod et al. proclaimed that the 98% of neodymium (III) was transferred by HFSLM at pH 4.5 using PC88A as carrier. H_2SO_4 1 M as the stripping solution was enough to recover 95% of the loaded Nd [13]. Using the same extractant, Pei et al. reported that Dy(III) can be selectively transported from a REEs solution in HCl media by a strip dispersion hollow fibre liquid membrane obtaining a better stability than traditional HFSLM [14]. Since the organic mass transfer coefficient (k_m = 0.788 cm·s^{-1}) was higher than the aqueous one (k_i = 0.0103 cm·s^{-1}) using Cyanex 272 as carrier by HFSLM, Wannachod et al. concluded that the diffusion of the praseodymium ions through the stagnant boundary layer between the feed solution and liquid membrane is the one which controls the process [15]. Furthermore, Ramakul et al. showed that the percentages of extraction and stripping of yttrium increase when TBP is added to Cyanex 272 due to the synergistic effect of the extractants using nitric acid as stripping solution by HFSLM, [16]. Yadav et al. demonstrate that the separation and purification of Dy(III) from NdFeB magnets scrap using EHEHPA as the extractant by a two- cycle hollow fibre membrane operation can be successfully achieved working in non-dispersive solvent extraction mode [17].

In recent years, the use of ionic liquids (ILs) have attracted attention as an alternative to the molecular solvents due to their unique properties. N,N-dioctyldiglycol amic acid (DODGAA) was synthetized by Kubota and Goto obtaining the advantages of neutral (extraction efficiency and REEs selectivity) and acidic extractants (high stripping yields) to the REEs separation [4,18]. It was demonstrated by using SLM system that DODGAA dissolved in the [C_4mim][Tf_2N] not only the REEs selectively separation from other metals such as Zn contained in cathode ray tubes was achieved [4], but also the stability of the liquid membrane, withstanding a long-term operation was shown [18].

Despite the amount of research using hollow fibre membranes to recover and separate REEs, only a few investigations use this technique in a complete separation process. The added value provided by this investigation is focused on the implementation of a membrane step to completely recover REEs in a process that can be industrially implemented.

In a previous article, a process to recover REEs from YOX fluorescent lamp wastes was proposed [19]. The end-of-life product was the main raw material, treated in a first leaching (L1) with nitric acid 1 M to separate non-ferrous impurities, mainly calcium. Then, the solid obtained after the L1 was undergone to a second

leaching (L2) using 2 M of nitric acid for the REEs recovery. Unfortunately, a small amount of these metals was also washed-up into the liquid fraction of the L1 stage. In order to minimize these losses, a SLM step was added. The purpose of the current research is to improve and increase the efficiency of this membrane step by using hollow fibre modules. Therefore, the entire process can be implemented at industrial scale to recover and separate REEs from non-REEs.

Pavón et al. reported that at high Cy923 concentrations a reduction of the metal transport was observed [19]. To elucidate this fact, a modifier has been added to the organic phase and this study examines the effect of the dynamic viscosity on the diffusion coefficient. Furthermore, this paper proposes a transport model for yttrium and europium using the permeability coefficient as the characteristic parameter including the correlation to the three main operating parameters: Cy923 concentration, modifier percentage (v/v) and viscosity of each mixture. The proposed model minimizes the efforts on the membrane process optimization, since determining the optimal conditions experimentally is laborious and time-consuming.

To sum up, the membrane step on the REEs recovery from the fluorescent lamp wastes has been substantially improved using hollow fibre modules working with renewal liquid membrane configuration.

2. Experimental methods

2.1. Reagents

Cyanex 923 was supplied by Cytec Canada Industries and used as received. Tributylphosphate (TBP, Ref. 240494) from Sigma Aldrich and 2,6-dimethylheptan-4-one (ONE, Ref. L16015) from Alfa Aesar were utilized as modifiers. Kerosene (Ref. 329460) and Na_2EDTA (Ref. E4884) from Sigma-Aldrich were used as diluent and stripping agent, respectively. Detailed specifications of the compounds are summarized in Table 1.

Table 1. Physical properties of the organic compounds.

Commercial Name	Content %	Density (25ºC) kg·m^{-3}	Viscosity (25ºC) mPa·s*	Av. Mol. Weight g·mol^{-1}
Cyanex 923 [20]	93	880	38.28	348
Tributylphosphate [21]	100	970	3.28	266.32
2,6-dimethylheptan-4-one [22]	92.8	809	0.94	142.24
Kerosene	100	800	1.64	

*Viscosity determined using an Ostwald's viscometer (Type 509 04. Ref. 285404014 from Schott Geräte GmbH)

The acidic leachate (L1) from fluorescent lamp wastes was obtained following the procedure depicted in Pavón et al. and was used as the feed solution. Its composition is shown in Table 2 [19].

Table 2. Composition of the feed solution after HNO_3 1 M leaching and contact time for 10 min [19].

	Element	mg·L^{-1}
Non-REEs	Ca	6820±150
	P*	759±14
	Fe	41±8.5
	Ba	311±0.1
	Sr	236±5.6
	Mn	152±3.5
	Si	132±3.1
	Al	116±2.5
	Na	90±2.1
	Mg	64±1.7
	K	56±1.4
	Sb	20±0.6

REEs	Y	491±12.2
	Eu	41±0.9
	La	16±0.3
Total REEs		548±6.6

* by molybdenum blue method [23]

2.2. FSSLM transport

The liquid membrane required a support to hold the carrier between the feed and the receiving solution. The support in this kind of membranes must be a hydrophobic and porous material with high chemical resistance against the organics utilized. The support of the FSSLM is impregnated with the carrier and placed between the feed and the receiving cells. Table 3 shows the characteristics of the polymeric support used in these experiments. They were carried out using the same experimental set-up as depicted by Pavon et al. [24].

Table 3. Characteristics of the microporous polytetrafluoroethylene film (Fluoropore™ FHLP04700, Merck Millipore).

Material	PTFE
Diameter (cm)	4.7
Pore diameter (μm)	0.45
Thickness (μm)	150*
Effective area (m^2)	11.4
Porosity (%)	85

*including 100 μm of the polyethylene grid

The feed cell was filled with 210 mL of the L1 leachate at pH=1, Cy923 diluted in kerosene was the carrier and 210 mL of Na_2EDTA 0.05 M was used as the stripping agent in the receiving cell. Both aqueous solutions were mechanically stirred at 1000 rpm and room temperature (20±2ºC). Samples from feed and receiving cells were withdrawn every hour, up to 8 h, and the metal concentrations were quantified by atomic emission spectrometry using a 4100 MP AES System (Agilent Technologies) with an analytical error less than 5%.

Transported metal *(% Me)* was the parameter used to evaluate the obtained results and can be referred to the feed or the receiving cell by Eq. (1) as:

$$\%\, Me = \frac{[Me]_{0,f} - [Me]_{t,f}}{[Me]_{0,f}} \cdot 100 = \frac{[Me]_{t,r}}{[Me]_{0,f}} \cdot 100 \qquad (1)$$

where $[Me]_{0,f}$ and $[Me]_{t,f}$ refer to the initial and at time *t* REE concentrations in the feed solution and $[Me]_{t,r}$ is the REE concentration at time *t* in the receiving solution.

2.3. HFRLM transport

The transport experiment was carried out using a hollow fibre module from Liqui-Cel™ (G-502) whose characteristics are provided in Table 4.

Table 4. Details of hollow fibre membrane module (G-502 from Liqui-Cel™).

Module diameter (cm)	7.7
Module length (cm)	27.7
Cartridge configuration	Extra-glow with center baffle
Membrane surface area (m^2)	1.4
Porosity (%)	40

OD/ID (μm)	300/200
Membrane/plotting material	PP/PE
Hold-up volume shell side (cm^3)	400
Hold-up volume lumen side (cm^3)	150

The lab-scale plant worked with 4 L of the feed solution containing 491 $mg \cdot L^{-1}$ of Y(III) and 41 $mg \cdot L^{-1}$ of Eu(III), from the L1 leachate. The pseudo-emulsion containing stripping/organic was made up of 400 mL of Na_2EDTA 0.05 M and 50 mL of organic phase (Cy923 diluted in kerosene) according to the low O:A ratios (organic-aqueous stripping ratios) suggested in the literature [9]. The feed and stripping/organic streams flowed at 50 $L \cdot h^{-1}$ and a low transmembrane pressure (P_f - P_s = 0.2 bar) between shell and lumen side was applied to avoid the organic phase transfer to the feed phase. The transport experiments were carried out using the experimental set-up depicted in Rathore et al. research [25]. Samples from feed and receiving phases were withdrawn at regular time intervals and the metal concentrations in both aqueous phases were determined by atomic emission spectrometry. The percentage of each REE transported were obtained using the Eq. (1).

It is mandatory the total replacement of the organic phase present in the pores after each experiment, to work at the new carrier concentration. For this reason, the transmembrane pressure was changed to -1 bar in order to force the organic phase to cross the fibre pores to the feed flow. Since the total volume of the pores was about 50 mL, the pore liquid has been completely renewed and the membrane was ready for the next run when 150 mL of the organic phase appeared in the feed tank.

3. Transport model

The metal transport through the membrane includes three resistances: (1) diffusion resistance on the feed side, (2) diffusion through the liquid membrane and (3) diffusion resistance on the stripping side (Fig. (1)).

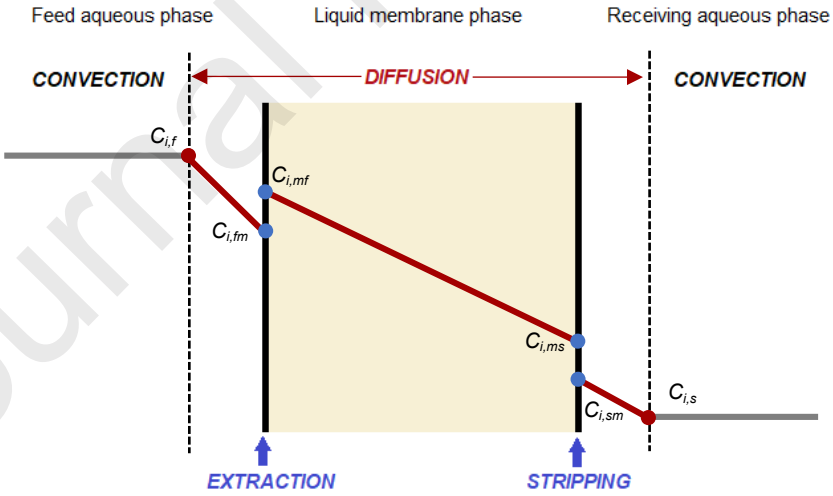

Fig. 1. Concentration profile for the REEs transport.

Taking into account that the stirrers in the cells are very close to the membrane in the FSSLM or the low O:A ratio when the HFRLM is used, the thickness of the boundary layer is minimized. For this reason, the resistance in the feed and stripping sides can be neglected. So, assuming instantaneous extraction and stripping reactions, it has been considered that the diffusion through the liquid membrane is the limiting step of the metal transport process.

The diffusion process is controlled by the 1st Fick's law.

$$J = -D \cdot \frac{dC_{i,m}}{dx} \quad (2)$$

where J is the diffusion REEs molar flux (mol REE/s · m^2), D is the diffusion coefficient (m^2/s), $C_{i,m}$ is the REE concentration in a point between both internal sides of the membrane (mol/L) and x is the position (m).

Discretizing the 1st Fick's law and applying it to the membrane, the Eq. (3) is obtained.

$$J = -D \cdot \frac{\Delta C_{i,m}}{\Delta x} = -D \cdot \frac{\Delta C_{i,m}}{\delta \cdot \tau} \quad (3)$$

where τ and δ are the tortuosity and the thickness (m), respectively.

On the other hand, the metal mass balance in the feed cell can be written as:

$$Acumulation = Input + Generation - Output - Consumption \quad (4)$$

Since there is no consumption and generation, and there is not input, the mass balance is simplified to:

$$Accumulation = -Output \quad (5)$$

where the accumulation can be expressed as the REE rate of change over time in the feed cell and the output as the mass flow of transferred REEs to the receiving phase (N_{REE}) expressed in mol/s.

$$\frac{dm_{i,f}}{dt} = -N_{REE} \quad (6)$$

The molar flow from the feed to the receiving phase is expressed as:

$$N_{REE} = J \cdot A_{eff} \quad (7)$$

Considering the porosity (ε), the effective transference area A_{eff} (m^2) can be written as:

$$A_{eff} = A \cdot \varepsilon \quad (8)$$

where A is the membrane area (m^2).

Replacing Eqs. (6)-(8) in Eq. (3):

$$\frac{dm_{i,f}}{dt} = V_f \cdot \frac{dC_{i,f}}{dt} = -D \cdot \frac{\varepsilon}{\delta \cdot \tau} \cdot (C_{i,mf} - C_{i,ms}) \cdot A \quad (9)$$

where V_f is the feed phase volume.

By the equilibrium extraction constant (K_{eq}), depicted in Eq. (10), it is possible to correlate the concentrations to the REE in the membrane/feed ($C_{i,mf}/C_{i,f}$) and the membrane/stripping ($C_{i,ms}/C_{i,s}$) interfaces.

$$K_{eq} = \frac{C_{REE,organic}}{C_{REE,aqueous} \cdot C_{carrier}} = \frac{C_{i,m}}{C_{i,p} \cdot C_{carrier}} \quad (10)$$

Being $C_{i,m}$ the concentration in the membrane at the feed or the stripping side, $C_{i,p}$ the concentration in the feed or the receiving phase and $C_{carrier}$ the concentration of the carrier.

The REEs neutral species concentration in the receiving phase, $C_{i,s}$, is maintained at zero because it is turned into an anionic species by EDTA complexation. Hence, considering the Eq. (10), the $C_{i,ms}$ is also zero. Thus, the Eq. (9) can be rewritten as:

$$\frac{dC_{if}}{dt} = -D \cdot \frac{\varepsilon}{\delta \cdot \tau} \cdot \frac{A}{V_f} \cdot C_{i,mf} \quad (11)$$

Considering the extraction equilibrium (Eq. (10)):

$$\frac{dC_{if}}{dt} = -D \cdot \frac{\varepsilon}{\delta \cdot \tau} \cdot \frac{A}{V_f} \cdot C_{i,f} \cdot K_{ex} \cdot C_{carrier} \quad (12)$$

Since the extraction equilibrium constants of both REEs, Y(III) and Eu(III), remain around 95% using 10%(v/v) of Cy923 diluted in kerosene or introducing TBP as well as ONE as modifiers, the K_{ex} can be considered as a constant parameter. Hence, Eq. (13) is obtained by grouping the support membrane characteristic parameters such as thickness, tortuosity and porosity, diffusion coefficient, extraction equilibrium constant and carrier concentration in a single variable.

$$\frac{dC_{i,f}}{C_{i,f}} = -P \cdot \frac{A}{V_f} \cdot dt \quad (13)$$

Being *P* the permeability coefficient (m/s) whose value refers to the speed with which the REEs from the feed phase are transported to the stripping phase.

Eq. (14) is obtained by integration of Eq. (13), and it is used to determine the REE permeability coefficient value for each specific concentration of carrier.

$$ln\frac{C_{i,f}}{C_{i,0,f}} = -P \cdot \frac{A}{V_f} \cdot t \quad (14)$$

where $C_{i,0,f}$ is the initial concentration of the REE in the feed phase.

3.1. Mathematical model

A mathematical model that allows predicting the evolution of the yttrium and europium metal ion concentrations in nitrate media using Cy923 as carrier has been developed. The *Matlab R2018a* software was used to solve the equations proposed relating the permeability coefficient to the concentration of carriers (Cy923 and ONE).

Is generally known that the diffusion coefficient (*D*) and the viscosity (μ) are the parameters which control the transport trough the membranes and they can be related through the Eq. (15):

$$D \cdot \mu^{\propto} = constant \quad (15)$$

where α is a coefficient with a value in the 0.5-1 range for this kind of liquid media [26,27].

To sum up, the diffusion process contemplates different parameters, some of them associated to the support membrane characteristics including the thickness, the porosity and the tortuosity, and others like viscosity which depends on the liquid membrane composition. Hence, the diffusion coefficient can be written as Eq. (16), considering that the support membrane characteristics are included in the permeability coefficient.

$$D = K \cdot \frac{P}{[Cy923]} \quad (16)$$

where *K* incorporates the membrane characteristics parameters (tortuosity, thickness and porosity).

Thus, the equation that permits to foresee the permeability coefficient of the REEs considering the membrane characteristics and the organic phase viscosity can be described by Eq. (17) as follows:

$$P = K' \cdot \mu^{-\alpha} \cdot [carrier] \quad (17)$$

where *K'* is the proportionality constant.

Assuming that the interactions between the Cy923, ONE and kerosene can be neglected, the viscosity of a mixture can be calculated from the viscosities of the individual components by using Eq. (18) [26,28].

$$\ln \mu_m = X_{Cy923} \cdot \ln \mu_{Cy923} + X_{ONE} \cdot \ln \mu_{ONE} + X_{kerosene} \cdot \ln \mu_{kerosene} \quad (18)$$

where μ_m is the viscosity of the mixture, $X_{Cy923,}$ X_{ONE} and $X_{kerosene}$ are the molar fractions and $\mu_{Cy923,}$ μ_{ONE} and $\mu_{kereosene}$ are the viscosities of each component in the ternary mixture. Firstly, the viscosities of the mixtures were measured using an Ostwald's viscometer and then, the Eq. (18) was validated by the experimental viscosities of different mixtures. Thus, the Eq. (18) was used to calculate the viscosities of any composition of the organic phase.

Considering that Cy923 and ONE, transport REEs, the permeability can be written as follows:

$$P = (K_{Cy923} \cdot [Cy923] + K_{ONE} \cdot [ONE]) \cdot \mu^{-\alpha} \quad (19)$$

The model depicted in the previous equations was used to obtain the optimized values of the proportionality constants, K_{Cy923} and K_{ONE}. The purpose is to find the parameter values that fit the calculated to the experimental data minimizing the error. The applied algorithm for the resolution of the model is shown in Fig. 2.

The resolution of the system starts with a matrix of the experimental data (15 experimental points), whose rows are the system conditions: concentration of Cy923 (0.3-1.2 M), ONE (0-40 %(v/v)) and kerosene and the experimental permeability coefficient (P_{exp}) from Eq. (14).

The theoretical viscosity of each organic phase (μ_m) was determined by using the Eq. (18). Then, the initialization of the proportionality constants (K_{Cy923} and K_{ONE}) is introduced and the P_{calc} was obtained by Eq. (19), taking into account the objective function $F(x)$ defined as the sum of the quadratic differences between the calculated and experimental permeability coefficients (Eq. (20)). This function was undergone to a minimization process using the *fmincon* subroutine. The standard deviation value (σ) was also evaluated following the Eq. (21) to quantify the dispersion of the calculated to experimental data.

$$F(x) = \sum_{i=1}^{N} (P_{i,calc} - P_{i,exp})^2 \quad (20)$$

$$\sigma = \sqrt{\frac{\sum_{i=1}^{N} (P_{i,calc} - P_{i,exp})^2}{N-1}} \quad (21)$$

where N is the number of experimental points.

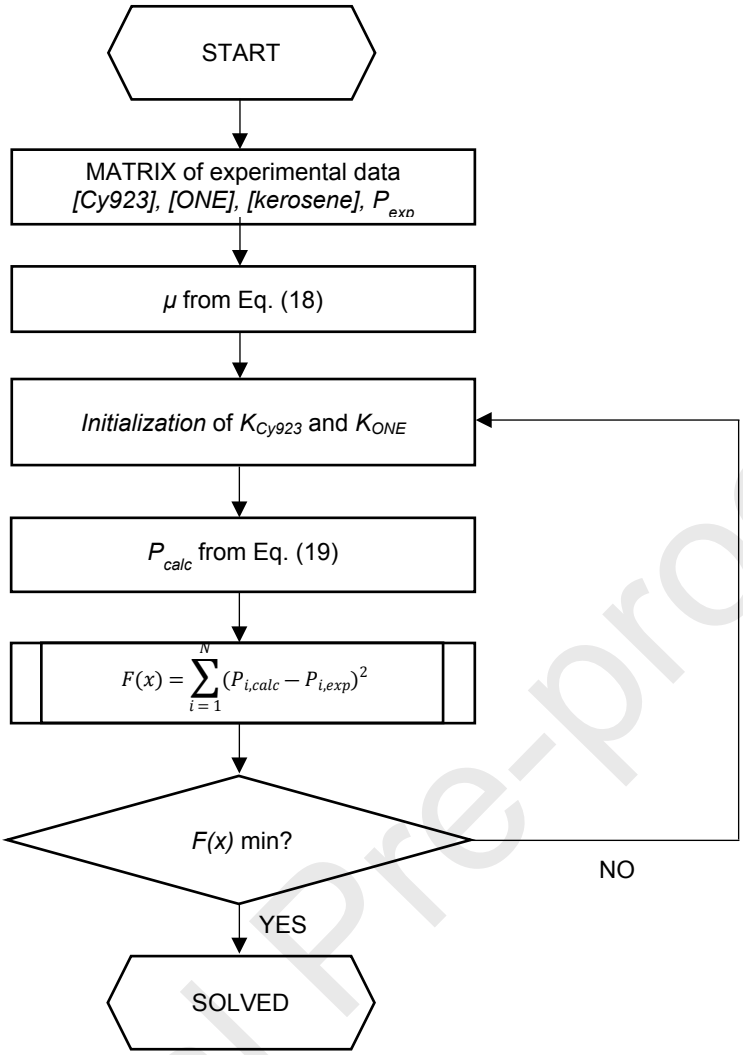

Fig. 2. Flow-sheet of the resolution algorithm.

4. Results and discussion

4.1. FSSLM transport

The leachate from the first leaching of the fluorescent lamp wastes was used as the feed solution for Y(III) and Eu(III) metal ions transport experiments using Cy923 as carrier by FSSLM. In a previous investigation published by Pavón et al. using the same system, it was observed that at low Cy923 concentrations, the metal ions transport is only controlled by the diffusion through the liquid membrane. In that respect, at higher Cy923 concentrations, the effect of the shear stress became predominant reducing thus, the permeability [19]. This decrease could be explained by the rise of the organic phase viscosity.

In order to elucidate it, two experiments using Cy923 1.2 M were carried out adding 20% of ONE or TBP as modifiers and the results are depicted in (Fig. 3).

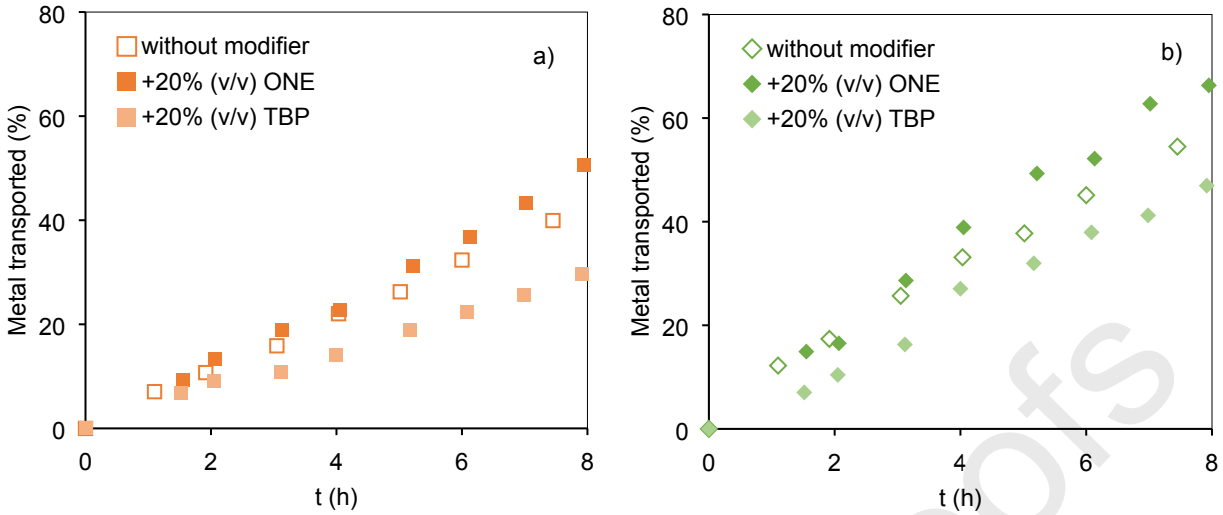

Fig. 3. Effect of the ONE or TBP addition in the organic phase on the REEs transport. [Cy923]=1.2 M. Feed: [Y(III)]=0.5 g·L^{-1}. [Eu(III)]=0.04 g·L^{-1}; pH=1.2. Receiving solution: 0.05 M Na_2EDTA. a) Y(III). b) Eu(III)

Comparing the obtained results, it can be asserted that the TBP has a negative effect on the transport and the permeability decreases due to the high viscosity value (Table 1). However, the REEs transport increases using ONE as modifier obtaining permeability coefficient values depicted in Table 5.

Table 5. Permeability coefficients of Y(III) and Eu(III) using 1.2 M of Cy923 and TBP or ONE as modifiers.

Modifier	**P ·10^6 (m·s^{-1})**	
	Y(III)	**Eu(III)**
-	3.31	5.03
TBP 20%(v/v)	2.11	3.81
ONE 20%(v/v)	4.03	6.67

To confirm the positive effect of the ONE on the REEs transport, a set of experiments using different Cy923 concentrations in the range of 0.3-1.2 M with 20% and 40% of the modifier were carried out. As shown in Fig. 4, the permeability coefficients increased when the modifier was added to the organic phase. The increases of these values for yttrium were around 18% and 33% when the percentage of the ONE was 20 and 40%, respectively, compared to the permeability values without ONE.

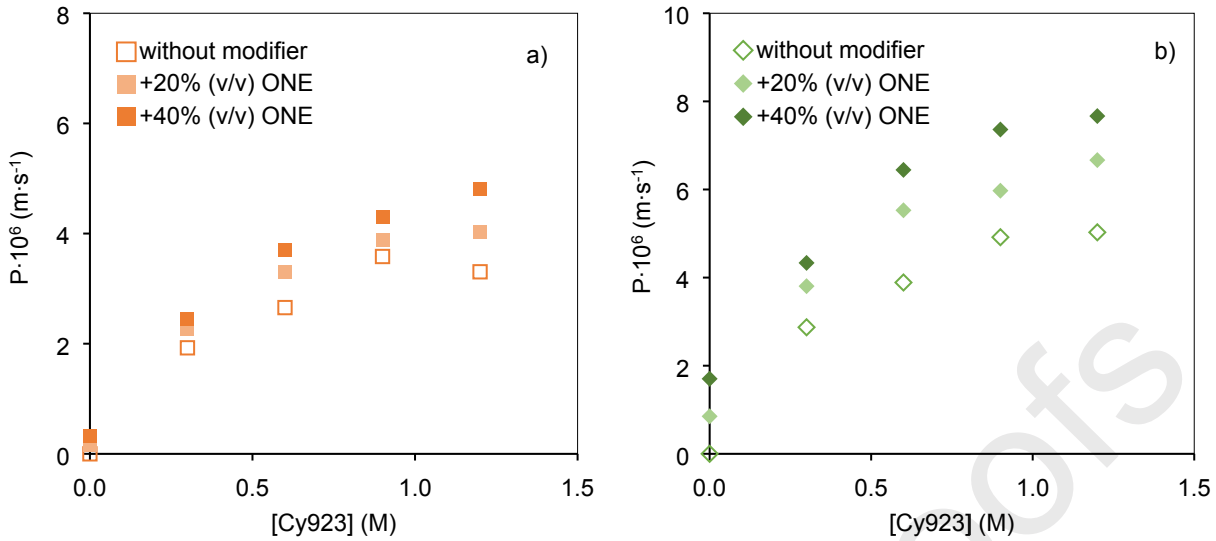

Fig. 4. Effect of the Cy923 concentration on the permeability of REEs using 20% or 40% of ONE as modifier. Feed: [Y(III)]=0.5 g·L^{-1}. [Eu(III)]=0.04 g·L^{-1}; pH=1.2. Receiving solution: 0.05 M Na_2EDTA. a) Y(III). b) Eu(III)

Consequently, a study of the dynamic viscosity effect on the diffusion coefficient was done following the procedure described in section 3.1. By this way, a linearization of Eq. (17) was used to obtain the results shown in Fig. 5.

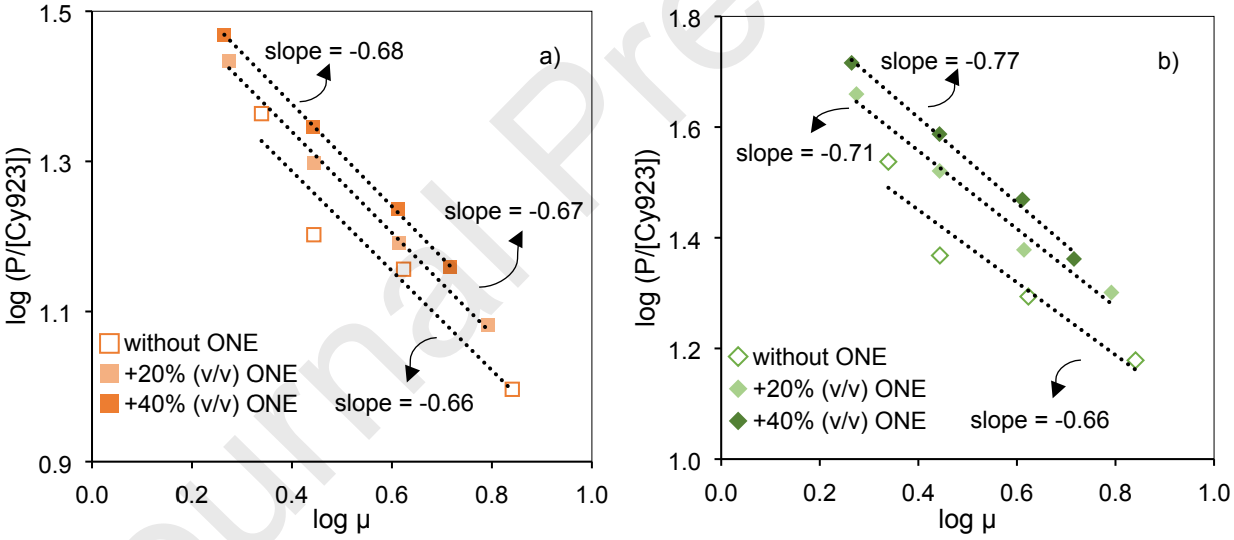

Fig 5. Effect of the dynamic viscosity on the diffusion coefficient. Feed: [Y(III)]=0.5 g·L^{-1}. [Eu(III)]=0.04 g·L^{-1}; pH=1.2. Receiving solution: 0.05 M Na_2EDTA. a) Y(III). b) Eu(III)

Eq. (22) proposed by Reid and Sherwood, Bird et al, Edward and Hildebrand [26,29–31] which described an inverse dependence between the diffusion coefficient and the viscosity, is commonly used. However, since the viscosities of the different concentrations of solvent studied are in a range of 1.8·to 6.9·mPa·s, the power for Y(III) and Eu(III) is very close to the (-2/3) power (Eq. (23)) according to Hiss and Cussler [27]:

$$D\cdot \mu^{1} = constant \quad (22)$$

$$D\cdot \mu^{2/3} = constant \quad (23)$$

As a result, the viscosity is responsible for the fact that the permeability remains practically constant or decreases at high Cy923 concentrations. Nevertheless, the ONE can be used as modifier in the organic phase, thus reducing the viscosity and obtaining higher permeability coefficients.

4.2. FSSLM model solving

To be able to predict the permeability coefficients for any concentration of Cy923 and ONE, the algorithm depicted in Fig. 2 has been applied. Proved by the experimental investigations that the power of the viscosity is close to 2/3, this value was used in the model. Hence, the optimized equations for yttrium and europium are:

$$P_{Y(III)} = (1.03 \cdot 10^{-5} \cdot [Cy923] + 8.06 \cdot 10^{-7} \cdot [ONE]) \cdot \mu^{-2/3} \quad (24)$$

$$P_{Eu(III)} = (1.47 \cdot 10^{-5} \cdot [Cy923] + 4.26 \cdot 10^{-6} \cdot [ONE]) \cdot \mu^{-2/3} \quad (25)$$

where P is in m·s^{-1}, *[Cy923]* in mol·L^{-1}, *[ONE]* in %(v/v) and μ in mPa·s.

The ionic radii of the heavy rare earths elements (HREEs) are smaller than the ones of light rare earths elements (LREEs) due to the lanthanide contraction and the higher charge density of Y(III) related to Eu(III) [32,33]. However, the permeability coefficient of europium is higher than the yttrium one, contrary to what was expected.

Nevertheless, this fact is according to the diffusion coefficient of Eu(III) being higher than the one of Y(III). Two individual transport experiments confirmed the findings, using the same concentration for both REEs (0.5·L^{-1}) containing 0.60 M of Cy923 and 20% of ONE in the organic phase. The results shown in Fig. 6 demonstrate that the permeability coefficient of Eu(III) is around 1.7 times higher compared to Y(III) ($P_{Eu(III)}$ = 2.37·10^{-2} and $P_{Y(III)}$ = 1.43·10^{-2} m·s^{-1}).

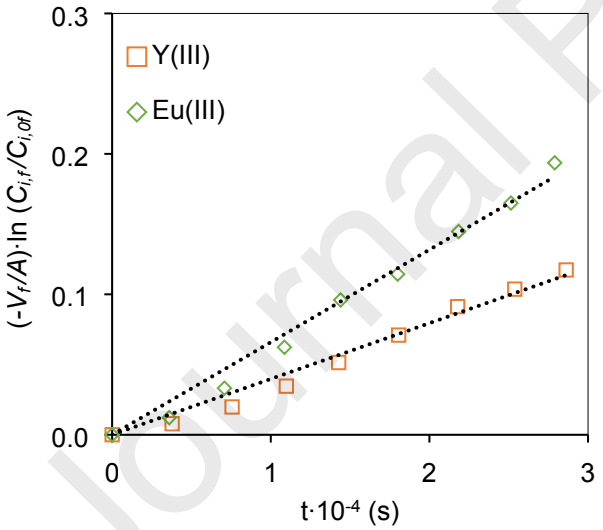

Fig. 6. REEs linear fitting of experimental data. Feed: [Y(III)]=[Eu(III)]=0.5 g·L^{-1}. pH=1.2. Receiving solution: 0.05 M Na_2EDTA. Organic phase: 0.60 M Cy923 and 20% of ONE.

Fig. 7 shows the permeability modelling results obtained in the 0-1.2 M Cy923 concentration range with an ONE range of 0-40%(v/v). The bold points are the experimental permeability data and the line corresponds to the local maximums. The proposed model is able to predict the permeability coefficient values for both REEs, obtaining low standard deviation values of 0.16 and 0.39 for Y(III) and Eu(III), respectively.

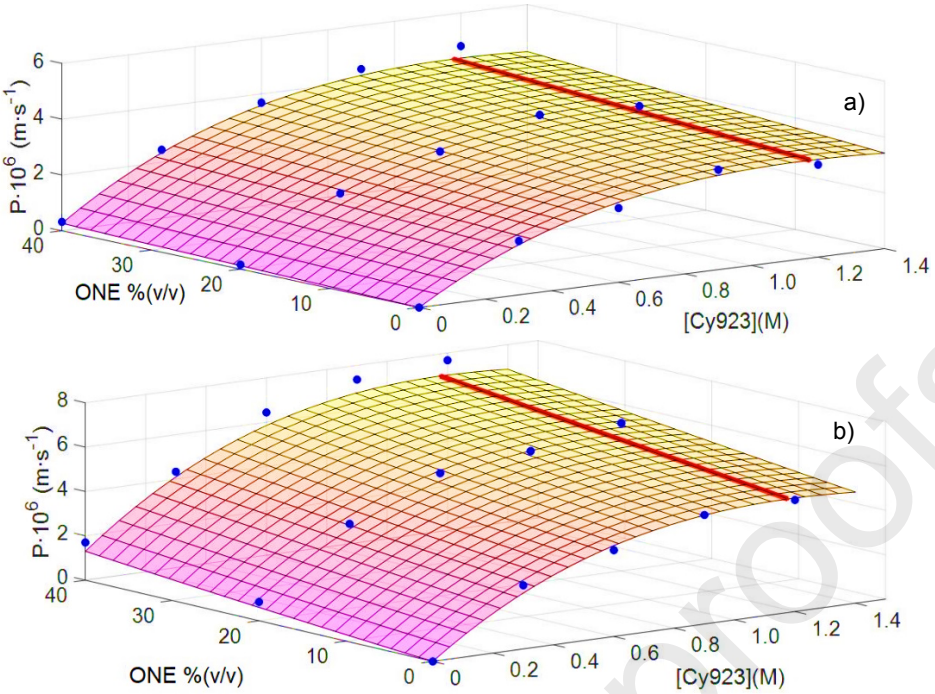

Fig. 7. Permeability coefficients calculated results vs. experimental ones varying the concentrations of Cy923 and ONE. Feed: [Y(III)]=0.5 g·L^{-1}. [Eu(III)]=0.04 g·L^{-1}; pH=1.2. Receiving solution: 0.05 M Na_2EDTA. a) Y(III). b) Eu(III)

The positive effect of the ONE addition to the organic phase is more significant at high concentrations of Cy923 because the viscosity is notably decreased when the ONE concentration increases. For this reason, the transport is considerably favoured using 40%(v/v) of ONE, reaching the maximum value of the permeability for both REEs. The optimal conditions for achieving the highest permeability coefficient value for Y(III) and Eu(III) are depicted in Table 6.

Table 6. Optimization parameters by using FSSLM.

REE	[Cy923] (M)	%(v/v) ONE	P·10^6 (m·s^{-1})
Y(III)	1.19	40	4.38
Eu(III)	1.18	40	7.00

4.3. HFRLM transport

To overcome the low area/volume ratio obtained using FSSLM, hollow fibre module was used to recover REEs from the L1 leachate. The feed flowed along the shell side of the module and to prevent organic solution losses from the membrane pores, a pseudo-emulsion containing the stripping phase and carrier flowed along the lumen side.

Although the optimization parameters obtained by using FSSLM should be used in the HFRLM to achieve the highest permeability coefficient values for both REEs, the experiments using HFRLM have been carried out without modifier owing to the chemical incompatibility of the ONE with the polypropylene material of the membrane fibres [34], Additionally, taking into account that 95% of REEs are transported after 2 h when the 0.3 M of Cy923 was used, a lower carrier concentration range (0.1-0.3 M) was studied instead of the optimal concentration range described in Table 5 to obtain the influences on the membrane process of this properties.

As can be seen in Fig. 8.a, 92% of Y(III) is transported after 4 h for whole range of Cy923 concentrations. The same trend is found for Eu(III), where 98% is transported (Fig. 8.b) due to its higher diffusion coefficient. The effect of the dynamic viscosity on the diffusion coefficient was studied (Fig. 8.c) to confirm that the

power is close to (-2/3). In addition, to verify that the permeability follows the same tendency obtained from the model by using FSSLM, the permeability coefficients for each experiment were determined and plotted in Fig. 8.d considering the (-2/3) power viscosity.

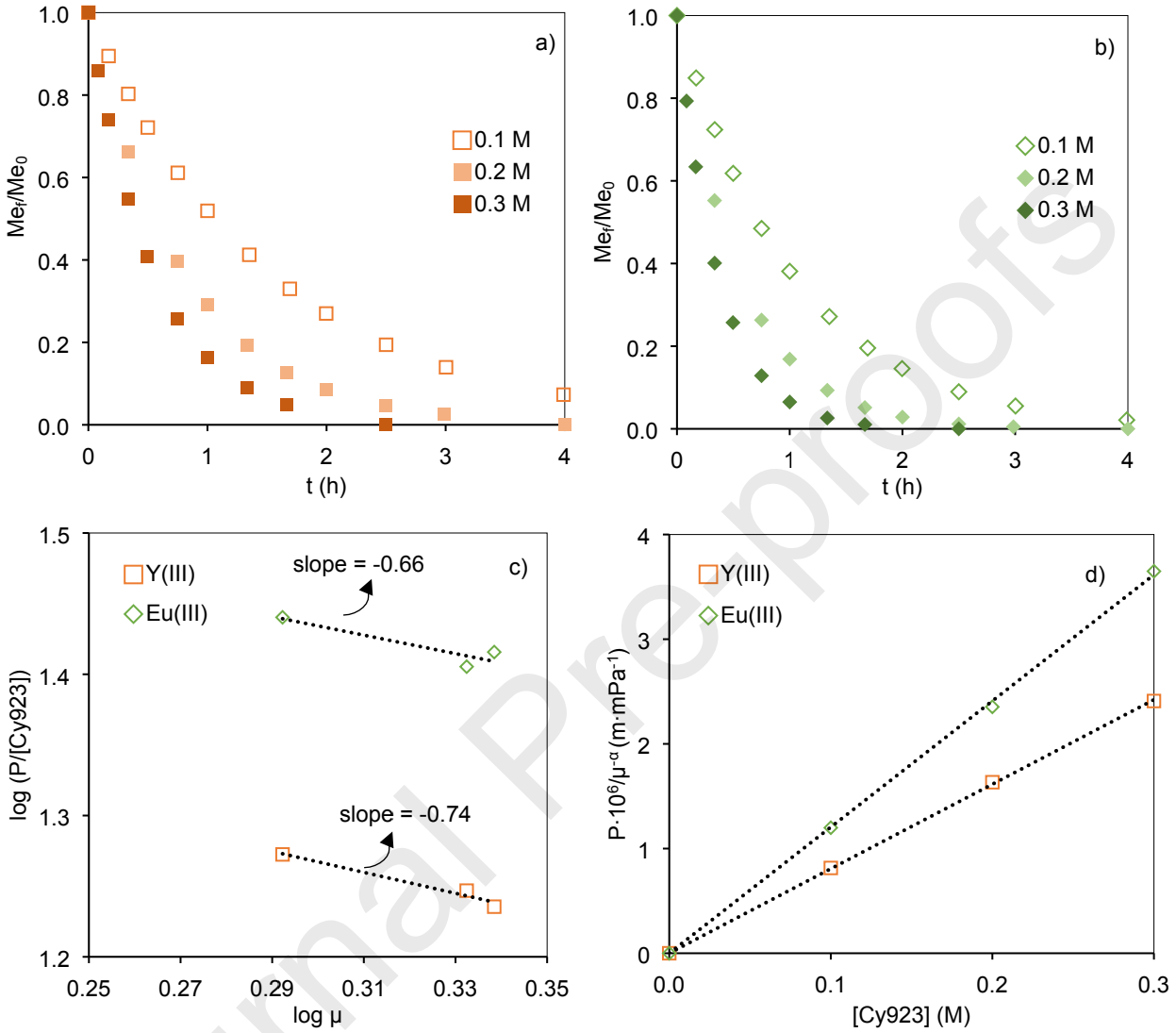

Fig. 8. Effect of Cy923 concentration on the REEs transport. [Y(III)]=0.5 g·L^{-1}. [Eu(III)]=0.04 g·L^{-1} a) Y(III). b) Eu(III). c) d) Effect of the Cy923 concentration on the permeability of the REEs.

As expected, for this Cy923 concentration range, the dependence on the permeability of the Cy923 concentration is linear. This proof the assumption, that the viscosity of the organic phase is not the parameter that restricts the REEs transport. Under these conditions, the transport process is controlled by diffusion, which can be expressed as linear equation relating the permeability to the carrier concentration (Eqs. (26)-(27)):

$$P_{Y(III)} = 8.08 \cdot 10^{-6} \cdot [Cy923] \cdot \mu^{-2/3} \quad (26)$$

$$P_{Eu(III)} = 1.20 \cdot 10^{-5} \cdot [Cy923] \cdot \mu^{-2/3} \quad (27)$$

where, as Eqs. (24)-(25), P is in m·s^{-1}, *[Cy923]* in mol·L^{-1} and μ in mPa·s.

4.4. FSSLM and HFRLM comparison

In order to justify the experimental permeability differences using FSSLM and HFRLM, and to confirm that these differences are due to the characteristics of the membranes [35–38], the permeability coefficient was calculated following the model depicted in Eqs. (24)-(25) and considering the (-2/3) power. Moreover, three experiments using a Cy923 concentration range of 0.1-0.3 M without ONE by using FSSLM were carried out to compare them with the results obtained from the HF module and also to assure that the experimental data fit with the model proposed. The linear dependence between the permeability and the carrier concentration is shown in Fig. 9 and the equations that relate both parameters can be seen in Eqs. (28)-(29) without ONE.

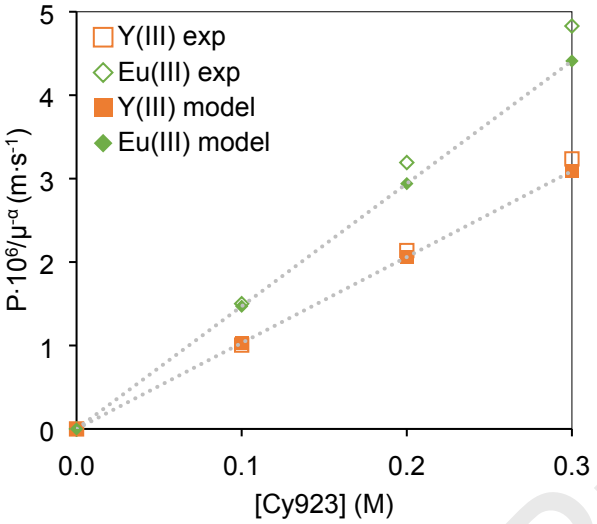

Fig. 9. Effect of the Cy923 concentration (without ONE) on the permeability of REEs using FSSLM. Feed: [Y(III)]=0.5 g·L^{-1}. [Eu(III)]=0.04 g·L^{-1}; pH=1.2. Receiving solution: 0.05 M Na_2EDTA.

Although the permeability coefficient for both membranes follows the same tendency, comparing the effect of the Cy923 concentration on the permeability of both membranes, it can be affirmed that the permeability coefficients using FSSLM are around 25% higher than using HFRLM. This value has to be the same for both REE since it is not dependent on the metal but only on the membrane characteristics.

$$P_{Y(III)FSSLM} = 1.27 \cdot P_{Y(III)HFRLM} \quad (28)$$

$$P_{Eu(III)FSSLM} = 1.23 \cdot P_{Eu(III)HFRLM} \quad (29)$$

The permeability coefficients of two different membranes can be related using the diffusion coefficient, the extraction equilibrium constant, the carrier concentration, the thickness, the tortuosity and the porosity (Eq. (13)). The tortuosity is the only structural parameter unknown for both membranes (Table 1 and Table 2). For the correlation of the permeability of both membranes, this characteristic parameter needed to be studied. Hence, considering the linear dependence of the permeability from the Cy923 concentration, Eq. (30) was obtained.

$$\tau_{FSSLM} = 1.28 \cdot \tau_{HFRLM} \quad (30)$$

where τ_{FSSLM} and τ_{HFRLM} are the tortuosity of the support of the FSSLM and HFRLM, respectively.

To confirm this relation between both different membranes, the tortuosity was also determined using Eqs. (31)-(32) [39–41].

$$\tau_{FSSLM} = A \cdot (1 - \varepsilon) + 1 \qquad \varepsilon \in [0.5 - 1] \quad (31)$$

$$\tau_{HFRLM} = B \cdot \frac{(1-\varepsilon)}{(\varepsilon - 0.33)^m} + 1 \qquad \varepsilon \in [0.4 - 0.5] \qquad (32)$$

where *A, B* and *m* are fitting parameters.

Using the *A, B* and *m* parameters shown in Table 7, the tortuosity relation between FSSLM to HFRLM is 1.24. The tortuosity values for both membranes are in accordance those found in the literature [42–44].

Table 7. Fitting parameters and tortuosity for both membranes.

	FSSLM	**HFRLM**
m	-	0.20
A	10	-
B	-	1.00
$\boldsymbol{\tau}$	2.50	2.02

To sum up, the permeability differences when the FSSLM and HFRLM are used, can be justified in terms of tortuosity, thickness and porosity differences.

4.5. Model solving for HFRLM

The mathematic model depicted in section 3.2 can be modified applying the 1.28 factor, mentioned in section 4.4, in the permeability equation obtained using FSSLM to have the correct permeability modelling when HFRLM are used. The Eqs. (33)-(34) are the optimized for yttrium and europium.

$$P_{Y(III)} = 8.24 \cdot 10^{-6} \cdot [Cy923] \cdot \mu^{-2/3} \qquad (33)$$

$$P_{Eu(III)} = 1.18 \cdot 10^{-5} \cdot [Cy923] \cdot \mu^{-2/3} \qquad (34)$$

where *P* is in m·s^{-1}, *[Cy923]* in mol·L^{-1} and μ in mPa·s.

Fig. 10 shows the permeability modelling using a Cy923 concentration range of 0-1.4 M. The bold points mark the maximums of the permeability values. While the calculated data fits the experimental ones standard deviation values for Y(III) and Eu(III) of 0.04 and 0.13, respectively, are achieved. Therefore, the proposed models for both REEs are able to predict the permeability coefficients. To achieve the maximum permeability value, the optimum Cy923 concentration is 1.18 (Table 8).

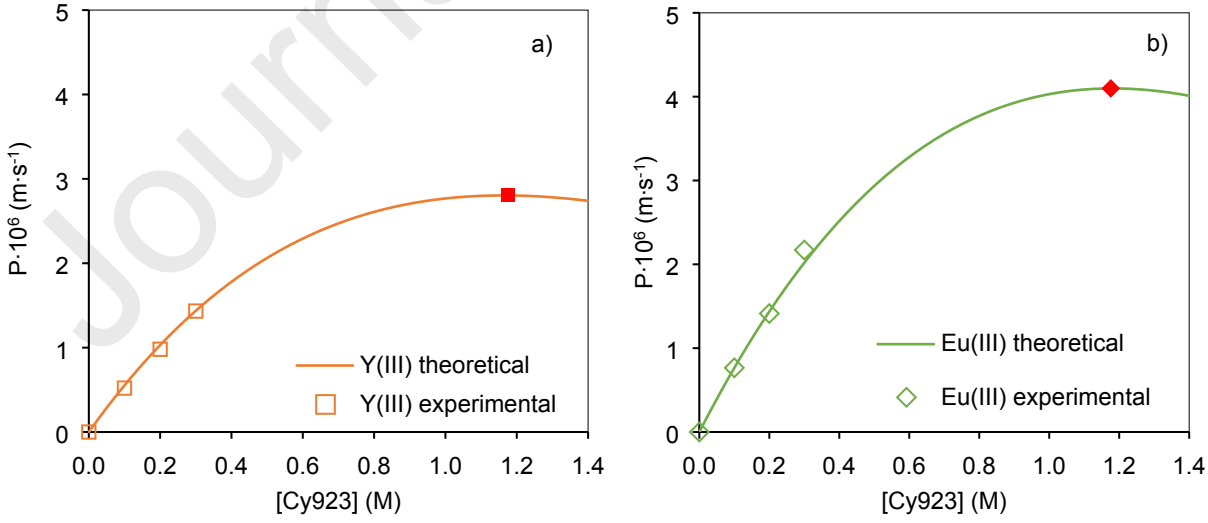

Fig. 10. Cy923 concentration effect on REEs permeability using HFRLM. Feed: [Y(III)]=0.5 g·L^{-1}. [Eu(III)]=0.04 g·L^{-1}; pH=1.2. Receiving solution: 0.05 M Na_2EDTA. a) Y(III). b) Eu(III)

Table 8. Optimization parameters by using HFRLM.

REE	[Cy923] (M)	$P \cdot 10^6$ ($m \cdot s^{-1}$)
Y(III)	1.18	2.80
Eu(III)	1.18	4.10

5. Conclusions

The recovery of Y(III) and Eu(III) through a membrane process depicted in a previous work [19] was investigated and successfully modelled. With the achieved increase in its efficiency, a basis for the implementation of the entire process at industrial scale is given.

The obtained results using two kind of membranes (FSSLM and HFRLM) reveal that the metal transport is only controlled by the diffusion through the membrane at low Cyanex 923 concentrations. However, the effect of the shear stress becomes predominant at higher concentrations of the carrier reducing the apparent permeability.

The transport model for Y(III) and Eu(III) was proposed to predict the permeability coefficients for both REEs depending on the Cyanex 923 and 2,6-dimethylheptan-4-one concentration and the organic phase viscosity. The results disclosed that the optimized parameters using FSSLM are 1.19 and 1.18 M of Cyanex 923 for Y(III) and Eu(III), respectively and 40% (v/v) of 2,6-dimethylheptan-4-one to achieve permeability coefficients of $4.38 \cdot 10^{-6}$ and $7.00 \cdot 10^{-6}$ $m \cdot s^{-1}$.

Due to the incompatibility of the 2,6-dimethylheptan-4-one with the polypropylene material of the HFRLM membrane fibres, it is not possible to use this phase modifier. In this case, the highest Y(III) and Eu(III) permeability coefficients, $2.80 \cdot 10^{-6}$ and $4.10 \cdot 10^{-6}$ $m \cdot s^{-1}$, respectively can be achieved by using 1.18 M of Cyanex 923.

Thus, the REEs recovery from the fluorescent lamp wastes has been considerably improved by using hollow fibre renewal liquid membranes.

Acknowledgements

This investigation was supported by the MINECO [grant number CTM2017-83581-R].

References

[1] A. Kumari, R. Panda, M.K. Jha, J.Y. Lee, J.R. Kumar, V. Kumar, Thermal treatment for the separation of phosphate and recovery of rare earth metals (REMs) from Korean monazite, J. Ind. Eng. Chem. 21 (2015) 696–703. doi:10.1016/j.jiec.2014.03.039.

[2] N.M. Ippolito, V. Innocenzi, I. De Michelis, F. Medici, F. Vegliò, Rare earth elements recovery from fluorescent lamps: A new thermal pretreatment to improve the efficiency of the hydrometallurgical process, J. Clean. Prod. 153 (2017) 287–298. doi:10.1016/j.jclepro.2017.03.195.

[3] C. Tunsu, M. Petranikova, C. Ekberg, T. Retegan, A hydrometallurgical process for the recovery of rare earth elements from fluorescent lamp waste fractions, Sep. Purif. Technol. 161 (2016) 172–186. doi:10.1016/j.seppur.2016.01.048.

[4] F. Kubota, M. Goto, Application of ionic liquids for rare-earth recovery from waste electric materials, Waste Electr. Electron. Equip. Recycl. (2018) 333–356. doi:10.1016/b978-0-08-102057-9.00012-3.

[5] L.L. Tavlarides, J.H. Bae, C.K. Lee, Solvent Extraction, Membranes, and Ion Exchange in Hydrometallurgical Dilute Metals Separation, Sep. Sci. Technol. 22 (1987) 581–617. doi:10.1080/01496398708068970.

[6] W.S.W. Ho, Removal and recovery of metals and other materials by supported liquid membranes with strip dispersion, Ann. N. Y. Acad. Sci. 984 (2003) 97–122. doi:10.1111/j.1749-6632.2003.tb05995.x.

[7] L. Chen, Y. Wu, H. Dong, M. Meng, C. Li, Y. Yan, J. Chen, An overview on membrane strategies for rare earths extraction and separation, Sep. Purif. Technol. 197 (2018) 70–85. doi:10.1016/j.seppur.2017.12.053.

[8] W.S. Winston Ho, B. Wang, T.E. Neumuller, J. Roller, Supported liquid membranes for removal and recovery of metals from waste waters and process streams, Environ. Prog. 20 (2001) 117–121. doi:10.1002/ep.670200215.

[9] F. Zahakifar, A. Charkhi, M. Torab-Mostaedi, R. Davarkhah, Performance evaluation of hollow fiber renewal liquid membrane for extraction of uranium(VI) from acidic sulfate solution, Radiochim. Acta. (2017). doi:10.1515/ract-2017-2821.

[10] L. He, L. Li, W. Sun, W. Zhang, Z. Zhou, Z. Ren, Extraction and recovery of penicillin G from solution by cascade process of hollow fiber renewal liquid membrane, Biochem. Eng. J. 110 (2016) 8–16. doi:10.1016/j.bej.2016.02.002.

[11] Z. Ren, W. Zhang, Y.M. Liu, Y. Dai, C. Cui, New liquid membrane technology for simultaneous extraction and stripping of copper(II) from wastewater, Chem. Eng. Sci. 62 (2007) 6090–6101. doi:10.1016/j.ces.2007.06.005.

[12] Z. Ren, W. Zhang, H. Meng, J. Liu, S. Wang, Extraction separation of Cu(II) and Co(II) from sulfuric solutions by hollow fiber renewal liquid membrane, J. Memb. Sci. 365 (2010) 260–268. doi:10.1016/j.memsci.2010.09.017.

[13] T. Wannachod, N. Leepipatpiboon, U. Pancharoen, S. Phatanasri, Mass transfer and selective separation of neodymium ions via a hollow fiber supported liquid membrane using PC88A as extractant, J. Ind. Eng. Chem. 21 (2015) 535–541. doi:10.1016/j.jiec.2014.03.016.

[14] L. Pei, L. Wang, W. Guo, Separation of Trivalent Samarium through Facilitated Stripping Dispersion Hollow Fiber Liquid Membrane Using p204 as Mobile Carrier, Chinese J. Chem. 29 (2011) 1233–1238. doi:10.1002/cjoc.201190229.

[15] P. Wannachod, S. Chaturabul, U. Pancharoen, A.W. Lothongkum, W. Patthaveekongka, The effective recovery of praseodymium from mixed rare earths via a hollow fiber supported liquid membrane and its mass transfer related, J. Alloys Compd. 509 (2011) 354–361. doi:10.1016/j.jallcom.2010.09.025.

[16] P. Ramakul, T. Supajaroon, T. Prapasawat, U. Pancharoen, A.W. Lothongkum, Synergistic separation of yttrium ions in lanthanide series from rare earths mixture via hollow fiber supported liquid membrane, J. Ind. Eng. Chem. 15 (2009) 224–228. doi:10.1016/j.jiec.2008.09.011.

[17] K.K. Yadav, M. Anitha, D.K. Singh, V. Kain, NdFeB magnet recycling: Dysprosium recovery by non-dispersive solvent extraction employing hollow fibre membrane contactor, Sep. Purif. Technol. 194 (2018) 265–271. doi:10.1016/j.seppur.2017.11.025.

[18] F. Kubota, J. Yang, M. Goto, Ionic Liquid-Based Extraction and the Application and Perspective of Ionic Liquids on Rare Earths Green Separation, 2012. doi:10.1080/01496395.2011.635171.

[19] S. Pavón, A. Fortuny, M.T. Coll, A.M. Sastre, Improved rare earth elements recovery from fluorescent lamp wastes applying supported liquid membranes to the leaching solutions, Sep. Purif. Technol. 224 (2019) 332–339. doi:10.1016/j.seppur.2019.05.015.

[20] CYTEC Industries Inc., CYANEX 923 Extractant. Technical Brochure, (2008).

[21] VWR We Enable Science, Tributylphosphat. Technical Brochure, 2018.

[22] Thermo Fisher Scientific, 2,6-dimethylheptan-4-one. Technical Brochure, 2018. doi:10.1016/j.jiec.2016.05.015.

[23] Z. He, C.W. Honeycutt, A modified molybdenum blue method for orthophosphate determination suitable for investigating enzymatic hydrolysis of organic phosphates, Commun. Soil Sci. Plant Anal. 36 (2005) 1373–1383. doi:10.1081/CSS-200056954.

[24] S. Pavon, M. Kutucu, M.T. Coll, A. Fortuny, A.M. Sastre, Comparison of Cyanex 272 and Cyanex 572 on the separation of Neodymium from a Nd/Tb/Dy mixture by pertraction, J. Chem. Technol. Biotechnol. (2017). doi:10.1002/jctb.5458.

[25] N.S. Rathore, A. Leopold, A.K. Pabby, A. Fortuny, M.T. Coll, A.M. Sastre, Extraction and permeation studies of Cd(II) in acidic and neutral chloride media using Cyanex 923 on supported liquid membrane, Hydrometallurgy. 96 (2009) 81–87. doi:10.1016/j.hydromet.2008.08.009.

[26] R.C. Reid, John M. Prausnitz, Bruce E. Poling, Properties of Gases and Liquids, Fourth, McGraw-Hill, 1958.

[27] T.G. Hiss, E.L. Cussler, Diffusion in high viscosity liquids, AIChE J. 19 (1973) 698–703. doi:10.1002/aic.690190404.

[28] V.A. Bloomfield, R.K. Dewan, Viscosity of liquid mixtures, J. Phys. Chem. 75 (1971) 3113–3119. doi:10.1021/j100689a014.

[29] R.B. Bird, W.E. Stewart, E.N. Lightfoot, Transport phenomena, J. Wiley, 2002. https://es.slideshare.net/Aapandove/bird-stewart-lightfoot-2002-transport-phenomena-2nd-ed (accessed January 20, 2019).

[30] J.H. Hildebrand, Motions of Molecules in Liquids: Viscosity and Diffusivity, Science (80-.). 174 (1971) 490–493. doi:10.1126/science.174.4008.490.

[31] J.T. Edward, Molecular volumes and the Stokes-Einstein equation, J. Chem. Educ. 47 (1970) 261–270.

[32] M. Gergoric, C. Ekberg, B.-M. Steenari, T. Retegan, Separation of Heavy Rare-Earth Elements from Light Rare-Earth Elements Via Solvent Extraction from a Neodymium Magnet Leachate and the Effects of Diluents, J. Sustain. Metall. 3 (2017) 601–610. doi:10.1007/s40831-017-0117-5.

[33] R. Banda, H.S. Jeon, M.S. Lee, Solvent extraction separation of La from chloride solution containing Pr and Nd with Cyanex 272, Hydrometallurgy. 121–124 (2012) 74–80. doi:10.1016/j.hydromet.2012.04.003.

[34] Graco, Chemicial Compatibility Guide, (2013).

[35] J.A. Currie, Gaseous diffusion in porous media. Part 2. - Dry granular materials, Br. J. Appl. Phys.

11 (1960) 318–324. doi:10.1088/0508-3443/11/8/303.

[36] N. Epstein, On tortuosity and the tortuosity factor in flow and diffusion through porous media, Chem. Eng. Sci. 44 (1989) 777–779. doi:10.1016/0009-2509(89)85053-5.

[37] L. Pisani, Simple Expression for the Tortuosity of Porous Media, Transp. Porous Media. 88 (2011) 193–203. doi:10.1007/s11242-011-9734-9.

[38] B. Ghanbarian, A.G. Hunt, R.P. Ewing, M. Sahimi, Tortuosity in Porous Media: A Critical Review, Soil Sci. Soc. Am. J. 77 (2013) 1461. doi:10.2136/sssaj2012.0435.

[39] A. Koponen, M. Kataja, J. Timonen, Permeability and effective porosity of porous media, Phys. Rev. E - Stat. Physics, Plasmas, Fluids, Relat. Interdiscip. Top. 56 (1997) 3319–3325. doi:10.1103/PhysRevE.56.3319.

[40] A. Koponen, M. Kataja, J. Timonen, Tortuous flow in porous media, Phys. Rev. E. 54 (1996) 406–410. doi:10.1103/PhysRevE.54.406.

[41] M. Matyka, A. Khalili, Z. Koza, Tortuosity-porosity relation in porous media flow, Phys. Rev. E - Stat. Nonlinear, Soft Matter Phys. 78 (2008) 1–8. doi:10.1103/PhysRevE.78.026306.

[42] R. Prasad, K.K. Sirkar, Dispersion-free solvent extraction with microporous hollow-fiber modules, AIChE J. 34 (1988) 177–188. doi:10.1002/aic.690340202.

[43] Š. Schlosser, I. Rothová, H. Frianová, Hollow-fibre pertractor with bulk liquid membrane, J. Memb. Sci. 80 (1993) 99–106. doi:10.1016/0376-7388(93)85135-J.

[44] A. Sengupta, R. Basu, K.K. Sirkar, Separation of solutes from aqueous solutions by contained liquid membranes, AIChE J. 34 (1988) 1698–1708. doi:10.1002/aic.690341014.

Author Contribution Statement

Author	CRediT Statement
Sandra Pavón	Methodology Software Validation Investigation Writing – Original Draft Writing – Review & Editing
Agustín Fortuny	Conceptualization Methodology Formal analysis Writing – Review & Editing Supervision
M. Teresa Coll	Conceptualization Methodology Writing – Review & Editing
Martin Bertau	Writing – Review & Editing
Ana M. Sastre	Resources Supervision Project administration Funding acquisition

Highlights

- Membrane step in REEs recovery process was improved to be industrially implemented
- REEs were completely recovered from fluorescent lamp leachates by using HFRLM
- Y(III) and Eu(III) can successfully transported by Cyanex 923 as a carrier
- The transport model relies on organic phase and support membrane characteristics

Declaration of interests

☒ The authors declare that they have no known competing financial interests or personal relationships that could have appeared to influence the work reported in this paper.

☐The authors declare the following financial interests/personal relationships which may be considered as potential competing interests: